

Active Contours: A Brief Review

Serdar Kemal Balcı and Burak Acar

Abstract—Active contours, also called snakes, are used extensively in computer vision and image processing applications, particularly to locate object boundaries. In this paper, we review and classify active contour models in literature. The paper first presents classical active contour models which use energy minimization techniques. We then review level set methods and present active contour models based on curve evolution and level set methods. We also discuss methods unifying energy minimization and curve evolution approaches and show the correspondence of level set methods to classical methods.

Index Terms—Active contours, level set methods, boundary extraction.

I. INTRODUCTION

Active contours, or snakes, as defined by Kass *et al.* [1] are curves defined within an image domain that can move under the influence of internal forces coming from within the curve itself and external forces computed from the image data. The essential idea is to evolve a curve or a surface under constraints from image forces so that it is attracted to features of interest in an intensity image. Snakes are widely used in many applications, including edge detection, shape modeling, segmentation, and motion tracking.

The active contour models in literature can be classified into two broad categories: parametric active contours [1], [3] and geometric active contours [4]–[9], [11]–[15]. In Kass *et al.*'s first efforts on active contours, the main idea was to formalize the problem as an energy minimization one. They defined active contours as energy-minimizing splines guided by external constraint forces that pull them toward features such as lines and edges. They also define an internal energy term which is used to impose a smoothness constraint on the moving curve. Because of the way the contours move while the energy is minimized they call them snakes. The classical active contour models due to Kass *et al.* had some drawbacks which were attempted to be solved by subsequent researchers. Two of its drawbacks was its failure to detect nonconvex objects and its sensitivity to initialization, which were partly solved by Xu and Prince [3] using the same energy minimization framework as Kass *et al.* However, the classical approach faced some more difficulties such as the need to

handle changes in topology of the active contour explicitly, the lack of a parametrization independent energy definition, numerical instabilities and resampling problems arising in solving the energy minimization problem.

Level set methods as introduced by Osher-Sethian [4] provided a framework in which new active contour models are formed which overcame the problems associated with classical energy minimization approaches. The level set formulation is based on the observation due to Osher-Sethian [4] that a curve can be seen as the zero level set of a function in higher dimension. Level set methods provide an efficient and stable algorithm to solve curve evolution equations. If the curve motion can be expressed as a velocity along the normal direction of the curve, level set methods are useful from several points of view. Firstly, changes in topology of the active contour are handled implicitly during the curve evolution. This is the main advantage of level set formulation as the topological changes should not be taken into account explicitly. Secondly, for numerical approximations, a fixed discrete grid in the spatial domain and finite-difference approximations for spatial and temporal derivatives can be used. A third advantage is that level set methods can be extended to any dimension which is not straightforward with the classical energy minimization schemes.

The geometric active contour models [4]–[9], [11]–[15] have made use of these advantages of level set formulation. Geometric active contour models are based on designing a speed term so that the evolving front gradually attains zero speed as it gets closer to the object boundaries and eventually comes to a stop. The speed term might depend on the boundary of the front while it can also make use of the information inside region enclosed by the evolving front. Beginning from Osher and Sethian's [4] level set formulation, Caselles *et al.* [5] and Malladi *et al.* [6] formulated their active contour model directly in terms of level sets. Caselles *et al.* [5] introduced geometric active contour model which was followed by Malladi *et al.* [6]. Caselles *et al.* [5] and Malladi *et al.* [6] designed a proper speed function so as to drive the evolving to the object boundaries. They provided a numerically stable and efficient model immune to topological changes. However, the stopping term was not robust and hence could not stop the leaking of the boundaries; and, if the front propagated and crossed the goal boundary, then it could not come back. Caselles *et al.* [7], [8] introduced geodesic active contours model which was based on minimizing an intrinsic weighted Euclidean length and showed its correspondence to Kass *et al.*'s classical snake model. Caselles *et al.* [7], [8] enhanced Caselles [5] and Malladi's

S. K. Balcı is with the Department of Electrical and Electronics Engineering at Bogazici University, Bebek, Istanbul, 34342, Turkey. (phone: (+90)-533-5706070; e-mail: serdar.balcı@gmail.com).

B. Acar is with the Department of Electrical and Electronics Engineering at Bogazici University, (e-mail: acarbu@boun.edu.tr).

model [6] by introducing an additional edge strength term. Aubert *et al.* [10] showed that geometric active contours unify the curve evolution framework with classical energy minimization techniques. Siddiqi *et al.* [11], [12] introduce an area based active contour model which minimizes a weighted area functional. Siddiqi *et al.* combine the weighted area minimizing flow with the weighted length minimizing flow of Caselles *et al.* [8] and Kichenassamy *et al.* [9]. They define an additional attraction force which can handle object boundaries having complex structures.

Boundary based level set methods provide efficient and stable algorithms to detect contours in a given image. They handle changes in topology and provide robust stopping terms to detect the goal contours. However, structures such as interior of objects, e.g. interior of discs are not segmented. Because of level set formulation the final contours are always closed contours. In addition, in images where the objects boundaries are noisy and blurry these methods face some difficulties. Some recent work in active contours by Chan and Vese [13], [14] consider these issues. The main idea is to consider the information inside the regions not only at their boundaries. Chan and Vese formulate their problem using area functionals and solve the problem using level set methods. A recent remark of Aubert *et al.* [17] claims that the region based functionals can be written as boundary based functionals. Hence, they show that region based active contour models, e.g. Chan and Vese's [14] are equivalent to boundary based active contour models.

We give our classification as follows. We divide active contour models into two broad categories: parametrized models and geometric models. We emphasize methods based on level set methods due to their aforementioned advantages. We classify geometric methods into two categories: models based on boundary functionals and models based on area functionals. We investigate models based on boundary functionals in detail and classify them according to the stopping term they use: image gradient based stopping functions, edge strength based stopping functions and weighed area gradient flow. We also present "active contours without edges" [14] as an example to models with area based functionals. In section II we investigate these methods in detail.

II. ACTIVE CONTOURS

A. Parametrized curves

1) Kass, Witkin, Terzopoulos model

Kass, Witkin and Terzopoulos gave the first efforts in formulating the boundary detection problem as an energy minimization one [1]. They define active contours, also called snakes, as energy-minimizing splines guided by external constraint forces that pull them toward features such as lines and edges. In Kass *et al.*, boundary detection consists in matching a deformable model to an image by means of energy minimization. Because of the way the contours move while

the energy is minimized they call them snakes. Let C be the set of curves in R^2 given by:

$$C = \{c : [a, b] \rightarrow \Omega, c \text{ piecewise } C^1, c(a) = c(b)\} \quad (1)$$

Using Aubert and Kornprobst's notation [2] for the formulation of Kass et al's active contour model, the energy functional $J(c)$ to be minimized is given by:

$$J(c) = \underbrace{\alpha \int_a^b |c'(q)|^2 dq + \beta \int_a^b |c''(q)|^2 dq}_{\text{Internal Energy}} + \underbrace{\lambda \int_a^b g^2(|\nabla I(c(q))|) dq}_{\text{External Energy}} \quad (2)$$

Where c' and c'' denote the first and second derivatives of c , respectively:

$$c(q) = (c_1(q), c_2(q)), \quad c'(q) = \left(\frac{dc_1}{dq}, \frac{dc_2}{dq} \right), \quad |c_1(q)| = \sqrt{\left(\frac{dc_1}{dq} \right)^2 + \left(\frac{dc_2}{dq} \right)^2} \quad (3)$$

and the same notation for c'' . $g(|\nabla I|)$ is a monotonic decreasing function satisfying the following condition:

$$g(0) = 1, \quad \lim_{s \rightarrow +\infty} g(s) = 0 \quad (4)$$

The function $g(|\nabla I|)$ is an edge detector function and a typical choice is:

$$g(|\nabla I|) = \frac{1}{1 + |\nabla I|^2} \quad (5)$$

$g(|\nabla I|)$ takes small values on edges and large values on smooth regions. The particular choice of $g(|\nabla I|)$ in (5) enhances contours in an image while reducing noise.

The first two terms in equation (2) are called internal energy and are used to impose a smoothness constraint. The first order term makes the curve act like a membrane and the second term makes it act like a thin plate. Setting $\beta = 0$ allows second order discontinuities as corners. Instead of being constant α, β can be selected to depend on the curve parameters as $\alpha(s), \beta(s)$ allowing the weight of smoothness constraints to change along the curve. The third term, called the external energy, attracts the curve toward the edges of the objects by taking smaller values at the object boundaries.

The Euler-Lagrange equations associated with $J(c)$ are a fourth order system:

$$\begin{cases} -\alpha c'' + \beta c^{(iv)} + \lambda \nabla F|_c(c) = 0 \\ c(a) = c(b) \end{cases} \quad (6)$$

Where $F(c_1, c_2) = g^2(|\nabla I(c_1, c_2)|)$.

In Kass *et al.*'s approach the main idea was to formulate the problem as a minimization one. However, this approach has significant drawbacks. One of the drawbacks is that the functional $J(c)$ is not intrinsic. It depends on the parametrization of c . Different solutions can be obtained by changing the parametrization while preserving the same initial curve. Another drawback is that the model cannot handle changes in topology. It is not possible to detect multiple objects. In addition nonconvex objects cannot be detected efficiently. A third consideration is about the numerical problems arising in solving equations in (6). In order to solve the system of equations in (6) the curve is made to depend on an artificial parameter t (the time) as follows:

$$\begin{cases} \frac{\partial c}{\partial t}(t, q) = -\alpha c'' + \beta c^{(iv)} + \lambda \nabla F|_c(c) \\ c(0, q) = c_0(q) \\ c(t, a) = c(t, b) \end{cases} \quad (7)$$

Since only a local minimum can be reached, $c_0(q)$ has to be chosen sufficiently close to the object to be detected. A difficult task is the choice of a set of marker points for discretizing the parametrized curve. The sampling rate of the markers has to be changed during iterations in order to avoid numerical instabilities and false detections.

2) Gradient Vector Flow (Xu and Prince)

Instead of defining an external energy and minimizing the energy functional $J(c)$ by solving the system of equations in (6) and (7), Xu and Prince [3] work directly on equations (6) and (7) and define an external force field that attracts the curve to boundaries. Xu and Prince [3] define a new static external force field $F_{ext} = \vec{v}(c)$, which they call the *gradient vector flow* (GVF) field. Replacing ∇F in (7) with $F_{ext} = \vec{v}(c)$ they obtain the following parametrized Euler-Lagrange equation:

$$\frac{\partial c}{\partial t}(t, q) = -\alpha c'' + \beta c^{(iv)} + \vec{v}(c) \quad (8)$$

Denoting $\nabla g(\nabla I)$ in (5) as an edge map, Xu and Prince investigate the properties of the edge map and try to design an edge map that has desirable features. The vectors in an edge map generally have large magnitudes only in the immediate vicinity of the edges. And in homogeneous regions, where ∇g is nearly constant, the vectors are nearly zero. Xu and Prince attempt to keep the highly desirable property of the gradients near the edges, but to extend the gradient map farther away from the edges and into homogeneous regions using a computational diffusion process.

Using the definitions in (1), (3) and (4) the gradient vector field is given to be the vector field $\vec{v}(c) = [u, v]^T$ minimizing the energy functional:

$$\varepsilon(c) = \int \mu \left(|\nabla u|^2 + |\nabla v|^2 \right) + |\nabla g|^2 \left| [u, v]^T - \nabla g \right|^2 dq \quad (9)$$

We can note that when ∇g is small, the energy in (9) is dominated by sum of the squares of the partial derivatives of the vector field, yielding a slowly varying field. On the other hand, when ∇g is large, the second term dominates the integrand, and is minimized by setting $\vec{v} = \nabla g$. This produces the desired effect of keeping \vec{v} nearly equal to the gradient of the edge map when it is large, but forcing the field to be slowly-varying in homogeneous regions. The parameter μ is a regularization parameter which should be set higher in noisy images.

The Euler-Lagrange equation associated with (9) is given by:

$$\mu \begin{bmatrix} \nabla^2 u \\ \nabla^2 v \end{bmatrix} - \left(\begin{bmatrix} u \\ v \end{bmatrix} - \nabla g \right) |\nabla g|^2 = 0 \quad (10)$$

Where ∇^2 is the Laplacian operator. In homogeneous regions $\nabla g = 0$ and the second term in (10) is zero. Within such a region \vec{v} is determined by Laplace's equation and the resulting GVF field is interpolated from the region's boundary. Therefore, GVF yields vectors that point into boundary concavities (See Figure 1). Equation (10) is solved numerically by discretization and iteration, similar to the Kass *et al.*'s method.

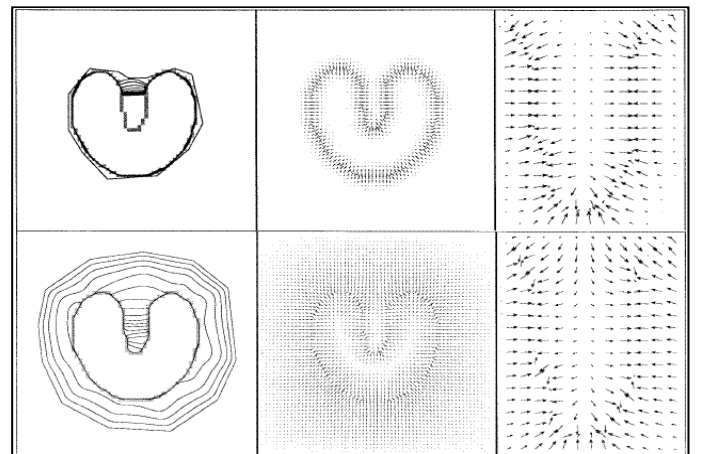


Figure 1: (From top left to bottom right) a) Convergence of a snake using b) potential forces in equation (7) c) shown close up within boundary concavity. d) Convergence of a snake using e) GVF external forces f) shown close up within boundary concavity [3].

Xu and Prince [3] tried to enhance Kass *et al.*'s method by introducing the gradient vector flow model. In comparison to Kass *et al.*'s model their model is less sensitive to initialization. This is achieved through a diffusion process that does not blur the edges themselves. In addition, their model can detect nonconvex objects. However, the main deficiencies in Kass *et al.*'s model are not solved. Problems about topological changes, parametrization dependency and numerical stability in Kass *et al.*'s model still persist in GVF snakes.

B. Geometric Models (Level Set Methods)

The equations (6) and (7) can be solved by parametrizing the curve c and discretizing the equations. However, this direct approach faces some numerical difficulties such as numerical instabilities and the need for sampling rate changes. Level set methods as introduced by Osher-Sethian [4] provide an efficient and stable algorithm to solve (6) and (7). The active contour models introduced in this part will make use of flows governed by equations of the form:

$$\begin{cases} \frac{\partial c}{\partial t} = FN \\ c(0, q) = c_0(q) \end{cases} \quad (11)$$

Equation (11) states that the curve $c(t, q)$ moves along its normal with a speed F , which may depend on t, c, c', c'' . The level set formulation is based on the observation due to Osher-Sethian [4] that a curve can be seen as the zero level set of a function in higher dimension. For example, a curve in R^2 can be represented as the zero-level line of a function $R^2 \rightarrow R$. Suppose that there exists a function $u : R^+ \times R^2 \rightarrow R$ such that

$$u(t, c(t, q)) = 0, \quad \forall q, \forall t \geq 0 \quad (12)$$

Then by differentiating (12) with respect to t :

$$\frac{\partial u}{\partial t} + \left\langle \nabla u, \frac{\partial c}{\partial t} \right\rangle = 0 \quad (13)$$

Setting the speed term in (11) into (13)

$$\frac{\partial u}{\partial t} + \langle \nabla u, FN \rangle = 0 \quad (14)$$

The unit normal is given as $N = -\frac{\nabla u}{|\nabla u|}$. Putting this into

(14):

$$\frac{\partial u}{\partial t}(t, c(t, q)) = F|\nabla u(t, c(t, q))| \quad (15)$$

This equation is valid only for the zero-level set of u . But, Osher-Sethian show in [4] that u can be regarded as defined on the whole domain $R^+ \times \Omega$. Then the following PDE can be solved

$$\frac{\partial u}{\partial t}(t, x) = F|\nabla u(t, x)| \quad (16)$$

For $t \geq 0$ and $x \in \Omega$ if F is defined on the whole space. Then once u is calculated on $R^+ \times \Omega$ the curve c can be obtained by extracting the zero level set of u . The normal derivative is chosen to vanish on the boundary and u is initialized to be the signed distance function to the initial curve c_0 . Then, Osher-Sethian give the following final model:

$$\begin{cases} \frac{\partial u}{\partial t}(t, x) = F|\nabla u(t, x)| & \text{for } (t, x) \in]0, \infty[\times \Omega \\ u(0, x) = \bar{d}(x, c_0) & (\bar{d} : \text{signed distance}) \\ \frac{\partial u}{\partial N} = 0 & \text{for } (t, x) \in]0, \infty[\times \Omega \end{cases} \quad (17)$$

If the curve motion can be expressed as a velocity along the normal direction of the curve, the model in (17) is useful from several points of view. Firstly, the evolving function $u(t, x)$ remains a function during evolution as long as F is smooth. However, the level set $u = 0$, so the front $c(t, q)$, may change topology, break, merge as u evolves. This is the main advantage of level set formulation as the topological changes should not be taken into account explicitly. Secondly, for numerical approximations, a fixed discrete grid in the spatial domain and finite-difference approximations for spatial and temporal derivatives can be used. A third advantage is that geometric elements of the front such as the normal vector and the curvature can be expressed with respect to u . In addition, level set methods can be extended to any dimension.

The following active contour models will make use of these advantages of level set formulation.

1) Models based on Boundary Functionals

Active contour models based on Osher-Sethian's level set formulation [4] are based on designing the speed function $F(t, c, c', c'')$ in (17) so that the evolving front gradually attains zero speed as it gets closer to the object boundaries and eventually comes to a stop. In addition, special stopping functions are designed in order to detect the contours more efficiently.

a) Image Gradient Based Stopping Functions

Beginning from Osher and Sethian's [4] level set formulation, Caselles *et al.* [5], proposed the geometric active

contour model which was followed by Malladi *et al.* [6]. The model proposed by Caselles and Malladi was based on equations (17), where they define a proper speed function F . The geometric active contour was given by solving:

$$\frac{\partial u}{\partial t} = \underbrace{g(|\nabla I|)}_{\text{stopping term}} \underbrace{(\kappa + \alpha)}_{\text{curvature + constant}} |\nabla u| \quad (18)$$

Where α is a constant and κ is the curvature, where:

$$\kappa = \text{div} \left(\frac{\nabla u}{|\nabla u|} \right) \quad (19)$$

The curvature term κ imposes smoothness constraints on the curve. The constant term α makes the detection of nonconvex objects easier and it increases the speed of convergence. In fact α is chosen so that $(\alpha + \kappa)$ remains of constant sign. In literature, the term α is sometimes called the balloon force. $g(|\nabla I|)$ is the stopping term which forces the evolving front to attain zero speed as it gets closer to the object boundaries. Caselles *et al.* [5] gives $g(|\nabla I|)$ as follows:

$$g(|\nabla I|) = \frac{1}{1 + |G_\sigma * \nabla I|} \quad (20)$$

Where $|G_\sigma * \nabla I|$ is the convolution of the gradient of the image with a Gaussian kernel of standard deviation σ .

Malladi defines $g(|\nabla I|)$ as

$$g(|\nabla I|) = e^{\gamma |G_\sigma * \nabla I|} \quad (21)$$

Where γ is some constant.

Caselles and Malladi formulated their active contour model directly in terms of level sets. Thereby, they provided a numerically stable and efficient model immune to topological changes. However, the stopping term was not robust and hence could not stop the leaking of the boundaries. The pulling back feature was not strong. This meant that if the front propagated and crossed the goal boundary, then it could not come back.

b) Geodesic Active Contours – Edge Strength based Stopping Function

Caselles *et al.* [7], [8] introduce geodesic active contours model which is based on minimizing an intrinsic weighted Euclidean length. Caselles *et al.* also show their models correspondence to Kass *et al.*'s classical snake model. Kichenassamy *et al.* [9] introduce an edge strength term to equation (18) which turns out to be in same form as Caselles *et al.*'s [8] geodesic active contour model. We first introduce

geodesic active contours model and shows its correspondence to Kass *et al.*'s snake model. Recalling the functional $J_1(c)$ and setting $\beta = 0$ in equation (2).

$$J_1(c) = \alpha \int_a^b |c'(q)|^2 dq + \lambda \int_z^b g^2(|\nabla I(c(q))|) dq \quad (22)$$

Aubert and Kornprobst [2] show that the term preceded by β is redundant and setting $\beta = 0$ also decreases the curvature of the curve. Caselles *et al.* introduce the functional $J_2(c)$ which is intrinsic, i.e. independent of parametrization:

$$J_2(c) = \int_a^b g(|\nabla I(c(q))|) |c'(q)| dq \quad (23)$$

If we compare $J_2(c)$ to the classical definition of a curve ($L = \int_a^b |c'(q)| dq$) we observe that $J_2(c)$ can be seen as a new

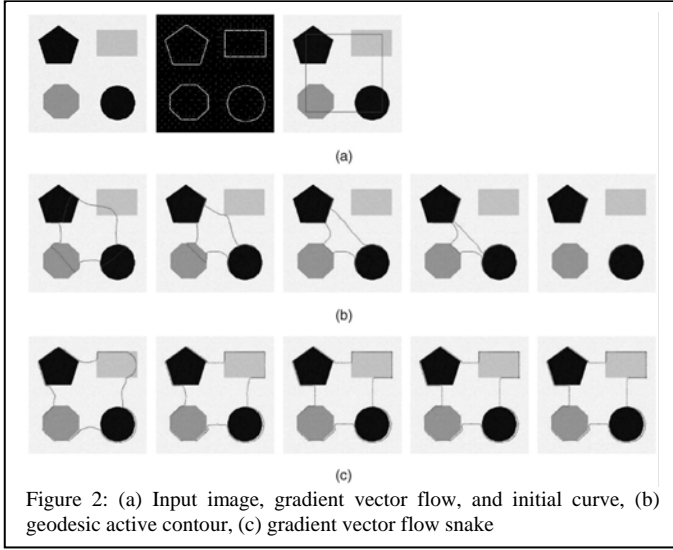
length by weighting the Euclidean length. The weight is $g(|\nabla I(c(q))|)$, which contains information regarding object boundaries. Caselles *et al.* define a new metric for which they seek for geodesic, hence the name geodesic active contours.

Aubert and Blanc-Feraud [10] provide a proof that minimizing $J_1(c)$ is equivalent to minimizing $J_2(c)$. Without going into details of the proof they state that the problems $\inf_c J_1(c)$ and $\inf_c J_2(c)$ are equivalent such that

the flow that most decreases for $J_1(c)$ is also a decreasing flow for $J_2(c)$ and vice versa. This explains the motivation behind choosing the functional $J_2(c)$. Thus, geometric active contours unify the curve evolution framework with classical energy minimization techniques, such as Kass *et al.*'s snakes. Caselles *et al.* [7], [8] and Kichenassamy *et al.* [9] arrive at the following level set expression:

$$\frac{\partial u}{\partial t} = g(|\nabla I|) (\kappa + \alpha) |\nabla u| + \underbrace{\langle \nabla g, \nabla u \rangle}_{\text{pull back term}} \quad (24)$$

This equation is similar to equation (18) and has an additional term $\langle \nabla g, \nabla u \rangle$, which attracts the curve further to the boundary. If the front propagates and crosses the goal boundary, this force pulls it back to the desired location. However, this method still suffers from boundary leaking for complex structures.



c) *Weighted area gradient flow*

Caselles *et al.* [7], [8] introduced geodesic active contours model which minimize a weighted Euclidean length. Similarly, Siddiqi *et al.* [11], [12] introduce an area based active contour model which minimizes a weighted area functional given by

$$A(c) = -\frac{1}{2} \int_0^L g(|\nabla I|) \langle c(s), N \rangle ds \quad (25)$$

Where L is the length of the curve, and $c(s)$ is the arc length parametrization of the curve and $g(|\nabla I|)$ is the weighting function as defined in (4). Then the area minimizing flow take the following form:

$$\frac{\partial c}{\partial t} = \left(g(|\nabla I|) + \frac{1}{2} \langle c, \nabla g(|\nabla I|) \rangle \right) N \quad (26)$$

The level set representation of area minimizing flow is given by:

$$\frac{\partial u}{\partial t} = \frac{1}{2} \operatorname{div} \left[\begin{pmatrix} x \\ y \end{pmatrix} g(|\nabla I|) \right] |\nabla u| \quad (27)$$

Where x and y are the (x, y) coordinates of the given image. Siddiqi *et al.* then combine the weighted area minimizing flow in (27) with the weighted length minimizing flow of Caselles *et al.* and Kichenassamy *et al.* in (24). The combined equation in level set form is given by

$$\frac{\partial u}{\partial t} = g(\kappa + \alpha) |\nabla u| + \langle \nabla g, \nabla u \rangle + \frac{\gamma}{2} \operatorname{div} \left[\begin{pmatrix} x \\ y \end{pmatrix} g \right] |\nabla u| \quad (28)$$

Where γ is a constant. The term $\operatorname{div} \left[\begin{pmatrix} x \\ y \end{pmatrix} g \right] |\nabla u|$

provides additional attraction force when the front is in the vicinity of an edge. Therefore, it performs better than geodesic active contours.

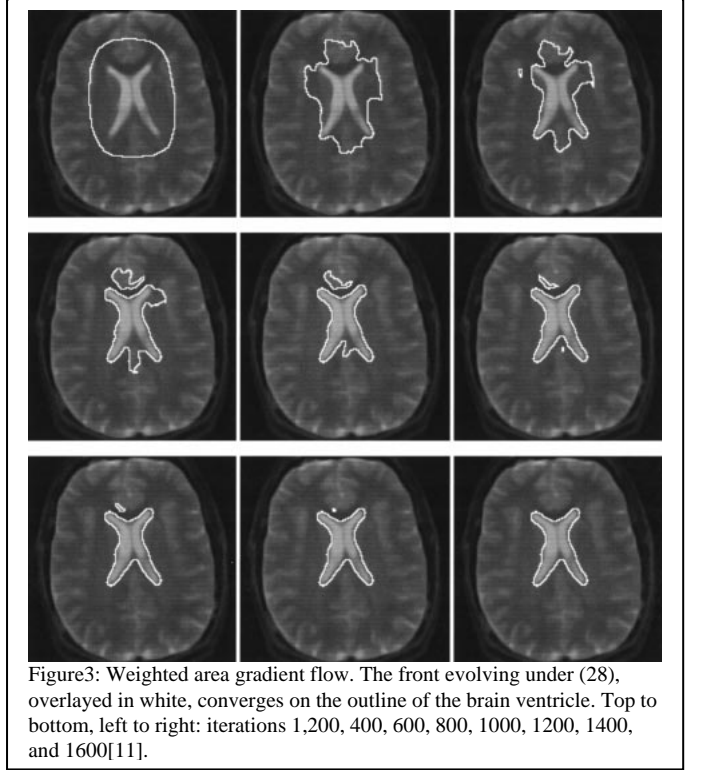


Figure3: Weighted area gradient flow. The front evolving under (28), overlaid in white, converges on the outline of the brain ventricle. Top to bottom, left to right: iterations 1,200, 400, 600, 800, 1000, 1200, 1400, and 1600[11].

2) Region Based Methods

Boundary based level set methods presented thus far provide efficient and stable algorithms to detect contours in a given image. The presented methods handle changes in topology and provide robust stopping terms to detect the goal contours. However, structures such as interior of objects, e.g. interior of discs are not segmented. Because of level set formulation the final contours are always closed contours. In addition, in images where the objects object boundaries are noisy and blurry these methods face some difficulties. Some recent works in active contours consider these issues.

a) *Active Contours without Edges*

There are some objects whose boundaries are not well defined through the gradient. For example, smeared boundaries and boundaries of large objects defined by grouping smaller ones (See Figure 5, 6). Chan and Vese introduce a new active contour model, called “without edges” [13], [14]. The main idea is to consider the information inside the regions not only at their boundaries. Chan and Vese define the following energy

$$\begin{aligned}
F(\phi, c_1, c_2) = & \underbrace{\mu \int_{\Omega} \delta(\phi) |\nabla \phi|}_{\text{length of } c} + \underbrace{\nu \int_{\Omega} H(\phi) dx dy}_{\text{area inside } c} \\
& + \underbrace{\lambda_1 \int_{\Omega} |u_0 - c_1|^2 H(\phi) dx dy}_{\text{fitting term I } (F_1(c))} \\
& + \underbrace{\lambda_2 \int_{\Omega} |u_0 - c_2|^2 (1 - H(\phi)) dx dy}_{\text{fitting term II } (F_2(c))}
\end{aligned} \quad (29)$$

Where u_0 is the original image, c_1, c_2 are some constants and $H(\phi)$ is given by:

$$H(\phi) = \begin{cases} 1 & \text{if } \phi \geq 0 \\ 0 & \text{if } \phi < 0 \end{cases} \quad (30)$$

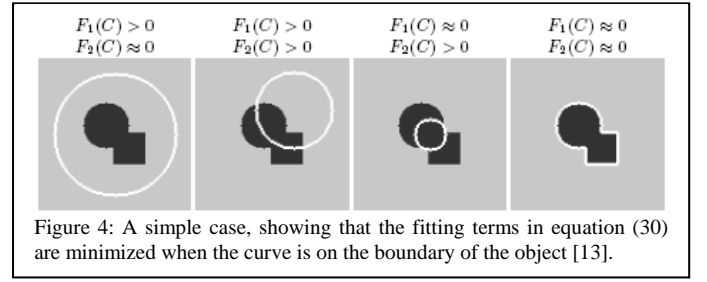
This model looks for the best approximation of image u_0 as a set of regions with only two different intensities (c_1 and c_2). One of the regions represents the objects to be detected (inside of c), and the other region corresponds to the background (outside of c). The snake c will be the boundary between these two regions. This model is related in spirit to the Mumford-Shah functional [15], which can be given as

$$\begin{aligned}
F_{MS}(c, u) = & \underbrace{\mu \text{length}(c) + \nu \text{area}(\text{inside}(c))}_{\text{fitting term}} \\
& + \int_{\Omega} |u - u_0|^2 dx dy
\end{aligned} \quad (31)$$

Where u is the cartoon image approximating u_0 , u is smooth except for jumps on the set C of boundary curves and the contour C segment the image into piecewise constant regions. The method in (29) is a simple approximation to (31) in that only two subregions are allowed in which u is piecewise constant. So u for (29) can be written as

$$u = c_1 H(\phi) + c_2 (1 - H(\phi)) \quad (32)$$

Returning to equation (29), the last two terms are fitting terms which guide the curve to the boundaries of the object. Figure 4 shows that the fitting terms $F_1(c)$ and $F_2(c)$ are minimized only at the object boundary. The first fitting term $F_1(c)$ gives the error resulting from approximating the original image inside c with c_1 and the second fitting term $F_2(c)$ gives the error resulting from approximating the original image outside c with c_2 .



The solution can be obtained by approximating $H(\phi)$ and $\delta(\phi)$ and by solving the following three equations

$$\begin{aligned}
c_1 &= \frac{\int_{\Omega} u_0 H(\phi) dx}{\int_{\Omega} H(\phi) dx} \quad (\text{average of } u_0 \text{ inside } c) \\
c_2 &= \frac{\int_{\Omega} u_0 (1 - H(\phi)) dx}{\int_{\Omega} (1 - H(\phi)) dx} \quad (\text{average of } u_0 \text{ outside } c) \\
\frac{\partial \phi}{\partial t} &= \delta(\phi) \left(\mu \text{div} \left(\frac{\nabla \phi}{|\nabla \phi|} \right) - |u_0 - c_1|^2 - |u_0 - c_2|^2 \right)
\end{aligned}$$

Where the last term is the Euler-Lagrange equations of equation (29). Figure 5-7 present some examples of active contours without edges.

Aubert *et al.* [17] show that the region based functionals can be written as boundary based functionals. Hence, they show that region based active contour models, e.g Chan and Vese's [14] active contours without edges, are equivalent to boundary based active contour models.

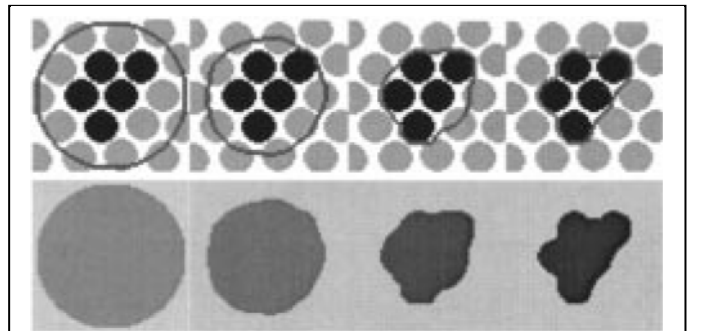


Figure 5: The boundary of a large object found by grouping smaller ones [13].

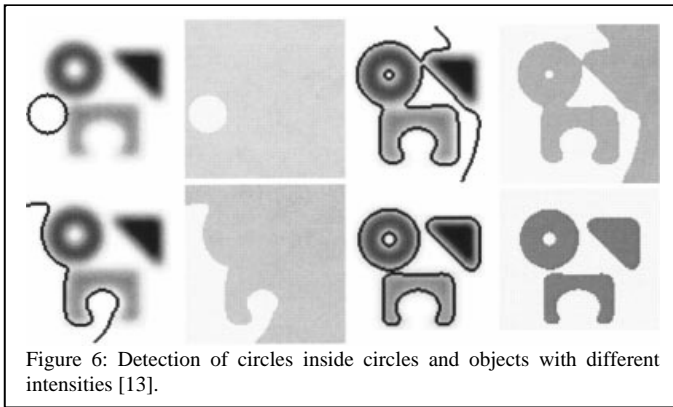


Figure 6: Detection of circles inside circles and objects with different intensities [13].

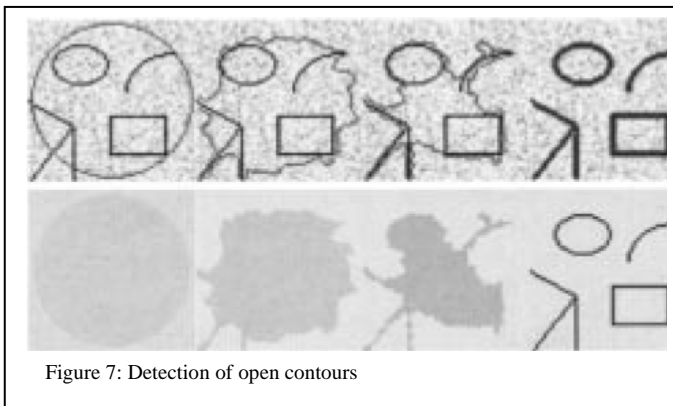


Figure 7: Detection of open contours

REFERENCES

- [1] M. Kass, A. Witkin, D. Terzopoulos, "Snakes: Active contour models," *International Journal of Computer Visio*, vol. 1, pp. 321-331, 1988.
- [2] G. Aubert and P. Kornprobst, *Mathematical Problems in Image Processing*, Germany: Springer Verlag, 2001, pp. 153-179.
- [3] C. Xu and J. L. Prince, "Snakes, Shapes, and Gradient Vector Flow," *IEEE Transactions on Image Processing*, vol. 7(3), pp. 359-369, 1998.
- [4] S.J. Osher and J.A. Sethian, "Fronts propagation with curvature dependent speed: Algorithms based on Hamilton-Jacobi formulations," *Journal of Computational Physics*, vol. 79, pp. 12-49, 1988.
- [5] V. Caselles, F. Catte, T. Coll, and F. Dibos, "A geometric model for active contours," *Numer. Math.*, vol. 66, no. 1, pp. 1-31, 1993.
- [6] R. Malladi, J. A. Sethian, and B. C. Vemuri, "Shape modeling with front propagation," *IEEE Trans. Pattern Anal. Machine Intell.*, vol. 17, pp. 158-175, Feb. 1995.
- [7] V. Caselles, R. Kimmel, and G. Sapiro, "Geodesic Active Contours," *Proc. IEEE Int'l Conf. Computer Vision*, pp. 694-699, 1995.
- [8] V. Caselles, R. Kimmel, and G. Sapiro, "On geodesic active contours," *Int. J. Comput. Vis.*, vol. 22, no. 1, pp. 61-79, 1997.
- [9] S. Kichenassamy, A. Kumar, P. Olver, A. Tannenbaum, and A. Yezzi, "Conformal curvatures flows: From phase transitions to active vision," *Arch. Rational Mech. Anal.*, vol. 134, no. 3, pp. 275-301, 1996.
- [10] G. Aubert, L. Blanc-Feraud, "Some remarks on the equivalence between 2D and 3D classical snakes and geodesic active contours," *International Journal Of Computer Vision*, 34(1), pp. 19-28, 1999.
- [11] K. Siddiqi, Y. B. Lauriere, A. Tannenbaum, and S. W. Zucker, "Area and length minimizing flows for shape segmentation," *IEEE Trans. Image Processing*, vol. 7, pp. 433-443, 1998.
- [12] K. Siddiqi, A. Tannenbaum, and S. W. Zucker, "Hyperbolic smoothing of shapes," *Proc. 6th Int. Conf. Comput. Vision (ICCV)*, vol. 1, pp. 215-221, 1998.
- [13] T. Chan and L. Vese, "An Active Contour Model without Edges," *Proc. Int'l Conf. Scale-Space Theories in Computer Vision*, pp. 141-151, 1999.
- [14] T. Chan and L. Vese, "Active contours without edges," *IEEE Trans. Image Processing*, vol. 10(2), pp. 266-277, 2001.
- [15] D. Mumford and J. Shah, "Optimal approximation by piecewise smooth functions and associated variational problems," *Commun. Pure Appl. Math.*, vol. 42, pp. 577-685, 1989.
- [16] S. Osher, R. Fedkiw, *Level Set Methods and Dynamic Implicit Surfaces*. New York: Springer Verlag, 2003, pp. 119-138.
- [17] G. Aubert, M. Barlaud, O. Faugeras, and S. Jehan-Besson, "Image segmentation using active contours: Calculus of variations or shape gradients?," *SIAM J. Appl. Math.*, vol. 63, pp. 2128-2154, 2003.